Physics Letters A 382 (2018) 1690–1694

Contents lists available at ScienceDirect

Physics Letters A

www.elsevier.com/locate/pla

Stationary states and rotational properties of spin–orbit-coupled Bose–Einstein condensates held under a toroidal trap

Zhang-Ming He [a], Xiao-Fei Zhang [b,d,*], Masaya Kato [c], Wei Han [b], Hiroki Saito [c]

[a] College of Science, Hunan University of Technology, Zhuzhou 412007, China
[b] Key Laboratory of Time and Frequency Primary Standards, National Time Service Center, Chinese Academy of Sciences, Xi'an 710600, China
[c] Department of Engineering Science, University of Electro-Communications, Tokyo 182-8585, Japan
[d] School of Astronomy and Space Science, University of Chinese Academy of Sciences, Beijing 100049, China

ARTICLE INFO

Article history:
Received 2 March 2018
Received in revised form 31 March 2018
Accepted 14 April 2018
Available online 19 April 2018
Communicated by R. Wu

Keywords:
Bose–Einstein condensate
Spin–orbit coupling
Toroidal trap

ABSTRACT

We consider a pseudospin-1/2 Bose–Einstein condensate with Rashba spin–orbit coupling in a two-dimensional toroidal trap. By solving the damped Gross–Pitaevskii equations for this system, we show that the system exhibits a rich variety of stationary states, such as vehicle wheel and flower-petal stripe patterns. These stationary states are stable against perturbation with thermal energy and can survive for a long time. In the presence of rotation, our results show that the rotating systems have exotic vortex configurations. These phenomenon originates from the interplay among spin–orbit coupling, trap geometry, and rotation.

1. Introduction

With the experimental realization of spin–orbit coupling (SOC) in neutral atomic gases, it has attracted enormous interest to explore the novel quantum state and its related dynamics [1–12]. The presence of SOC significantly changes the low-energy states of single particle Hamiltonian, and the highly degenerate single-particle ground state leads to the formation of a variety of novel quantum states, such as half-quantum vortex, fractionalized Skyrmion lattice, two-dimensional (2D) semi-vortex solitons, topological superfluidity, stripe phase, and so on [13–29]. Typically, the spin–orbit (SO) coupled Bose–Einstein condensates (BECs) with a harmonic trap shows a complex phase diagram, and two classes of phases and several subphases are identified [17–21].

One of the many remarkable new results from the study of ultracold gase is its rotational property, which manifest itself as the presence of quantized vortex and its related vortex lattice [30–32]. The typical vortex structures of a harmonically-trapped BECs with SOC and rotation have been well studied, showing various exotic vortex lattices by varying the strength of SOC and rotation frequency [33–38]. Recently, BECs in toroidal traps have been the subject of many experimental and theoretical investigations, where one can study the fascinating properties of a superfluid [39–54]. Very recently, we have considered the mean-field and quantum many-body ground states of a SO coupled BECs held under a toroidal trap, and found that the system exhibits a variety of ground-state structures, such as a modified stripe, an alternately arranged stripe, and countercircling states [55]. In addition, odd-petal states and persistent flows in SO coupled BECs have been investigated in Ref. [56].

In this paper, we focus on stationary states and rotational properties in a pseudospin-1/2 BEC subject to Rashba SOC held under a toroidal trap. We find that there exist parameter regimes in which the competition between the trap geometry and SOC is significant, which allows a rich variety of metastable stationary states, such as triangular stripes and flower-petal patterns. To show that such stationary states can be reached in experiments, we solve the damped Gross–Pitaevskii equation that describes time evolution of the system in realistic dissipative environment. We find that the stationary states can be reached from various initial states, and they are stable against perturbation with thermal energy. Furthermore, we also show that in the presence of external rotation the system exhibits exotic vortex configurations.

The paper is organized as follows. In Sec. 2, we present the model for describing the SO coupled BECs held under a toroidal trap and briefly introduce the numerical method. In Sec. 3, various stationary states and rotational properties of such a system are investigated using the mean-field theory. Finally, Sec. 4 provides our discussion and conclusions.

* Corresponding author at: Key Laboratory of Time and Frequency Primary Standards, National Time Service Center, Chinese Academy of Sciences, Xi'an 710600, China.
E-mail address: xfzhang@ntsc.ac.cn (X.-F. Zhang).

https://doi.org/10.1016/j.physleta.2018.04.032
0375-9601/

2. Formalism

The toroidal trap considered in this paper can be realized by a blue-detuned laser beam to make a repulsive potential barrier in the middle of a harmonic magnetic trap, and its radii and shape can be modified by changing the intensity and size of the plug beam [46]. The quasi-2D system can be realized by a tight harmonic potential with frequency $\omega_z \gg \omega_\perp$, where the longitudinal motion of the condensate is frozen to the ground state of the longitudinal harmonic trapping potential. Within the framework of mean-field theory, the Hamiltonian of such a system is given by $\mathcal{H} = \mathcal{H}_0 + \mathcal{H}_{\rm int}$, where

$$\mathcal{H}_0 = \int d\mathbf{r}\psi^\dagger \left[-\frac{\hbar^2\nabla^2}{2m} + \mathcal{V}_{so} + V(r) - \Omega L_z \right] \psi,$$
$$\mathcal{H}_{\rm int} = \int d\mathbf{r} \left(\frac{g_{\uparrow\uparrow}}{2}\psi_\uparrow^{\dagger 2}\psi_\uparrow^2 + \frac{g_{\downarrow\downarrow}}{2}\psi_\downarrow^{\dagger 2}\psi_\downarrow^2 + g_{\uparrow\downarrow}\psi_\uparrow^\dagger\psi_\downarrow^\dagger\psi_\downarrow\psi_\uparrow \right), \quad (1)$$

where $\psi = (\psi_\uparrow, \psi_\downarrow)^T$ denotes the field operator of the atom with pseudospin state $\uparrow, \downarrow$, and m is the atomic mass. The Rashba SOC is $\mathcal{V}_{so} = -i\kappa(\sigma_x\partial_x + \sigma_y\partial_y)$ with $\sigma_{x,y}$ being the Pauli matrices and κ is the strength of the SOC. Ω is the rotation frequency and L_z is the z-component of the orbital angular momentum, where we assume that the "SOC lasers" are also rotated with the system to simplify the problem [34]. The effective 2D interaction parameters are given by $g = \sqrt{8\pi}\hbar^2 a/(ma_z)$ and $g_{\uparrow\downarrow} = \sqrt{8\pi}\hbar^2 a_{\uparrow\downarrow}/(ma_z)$, where a and $a_{\uparrow\downarrow}$ are the corresponding s-wave scattering lengths and $a_z = \sqrt{\hbar/(m\omega_z)}$. To simplify the problem, here we further assume that the two intracomponent interaction parameters are the same, $g_{\uparrow\uparrow} = g_{\downarrow\downarrow} \equiv g$. The external potential considered in this work can be written as

$$V(r) = \frac{1}{2}m\omega_\perp^2 r^2 + V_0 e^{-2r^2/\sigma_0^2}, \quad (2)$$

where $\omega_\perp$ is the radial trap frequency of the harmonic potential, $r^2 = x^2 + y^2$, and V_0 and σ_0 are proportional to the intensity and beam waist of the optical plug. Such a type of external potential can be realized by superposing a central repulsive potential barrier onto a harmonic trap [46], or intersecting a red-detuned sheet laser and a laser using a ring-shaped Laguerre–Gaussian mode [57,43], or using a hybridmagnetic-optical trap where a target ring potential is imaged onto the condensate using an intensity mask [42].

To study stationary states to which the system evolves, we employ the damped Gross–Pitaevskii (GP) equation, which converges to the ground or stationary states and simulates the dynamics of actual experimental systems with energy dissipation [58]. The damped dimensionless GP equation can be obtained by replacing i with $i - \gamma$ on the left-hand side of the usual GP equation, and can be written as

$$(i-\gamma)\frac{\partial\psi_\uparrow}{\partial t} = \left(-\frac{\nabla^2}{2} + \mathcal{V}_{\rm so} + V(r) - \Omega L_z + g|\psi_\uparrow|^2 + g_{\uparrow\downarrow}|\psi_\downarrow|^2 \right)\psi_\uparrow,$$
$$(i-\gamma)\frac{\partial\psi_\downarrow}{\partial t} = \left(-\frac{\nabla^2}{2} + \mathcal{V}_{\rm so} + V(r) - \Omega L_z + g|\psi_\downarrow|^2 + g_{\uparrow\downarrow}|\psi_\uparrow|^2 \right)\psi_\downarrow, \quad (3)$$

where γ is a phenomenological damping parameter, and we set $\gamma = 0.01$ throughout this work. The results are not sensitive to the value of γ. Here we work in dimensionless units by introducing the scales characterizing the trapping potential: the length is expressed in units of oscillator length $\sqrt{\hbar/(m\omega_\perp)}$, the time is expressed in units of $1/\omega_\perp$, and the energy is expressed in units of oscillator energy $\hbar\omega_\perp$. Thus, the toroidal trap can be rewritten as

$$V(r) = r^2/2 + Ae^{-r^2/l^2}, \quad (4)$$

where $l = \sqrt{m\omega_\perp\sigma_0^2/(2\hbar)}$ and $A = V_0/(\hbar\omega_\perp)$. To reduce the number of parameters, we focus on the special case with $A = 100$ and varied l. In this case, the area of the central hole can be controlled by changing the parameter l. We start our numerical simulations of Eq. (3) from various initial states including the ground state without SOC with random noises. The stationary states are reached by solving Eq. (3) using the pseudospectral method with the fourth-order Runge–Kutta scheme.

3. Results and discussions

Without external potential or with a very weak harmonic trap, the ground state of a SO coupled system shows either a plane wave or a striped wave depending on the ratio between inter- and intra-component interactions [16]. In the presence of a regular 2D harmonic trap, the nontrivial interplay between SOC, external potential and contact interactions leads to a rich phase diagram comprising different ground phase structure, such as half-vortex, lattice phase, stripe phase, and so on [17,21]. In the presence of a toroidal trap, by varying the strength of SOC and the size of the central hole region, a SO coupled condensate held under a toroidal trap reveals a series of ground-state phases in the ground state of the system [55,56]. In what follows, we will perform a detailed numerical study of the stationary states and rotational property of such a system held under a toroidal trap.

3.1. Stationary states without rotation

We begin with the stationary states of such a system for both miscible and immiscible cases for $\Omega = 0$. Fig. 1(a) shows the density and flow patterns of a stationary state for the miscible case with $g = 1000$, $g_{\uparrow\downarrow} = 800$, $l = 3$, and $\kappa = 3$, where the direction of the phase gradient of $\psi_\uparrow$ is marked by the dashed-line arrows. The direction of the phase gradient of $\psi_\downarrow$ is the same as that of $\psi_\uparrow$. We recall that as the central hole of the toroidal trap is increased, the true ground state changes from the plane-wave state to the countercircling state, in which the wave number vectors align clockwise and counterclockwise on the two semicircles, and then changes to the one-way circling state [55]. The true ground state for the present parameter is the countercircling state. For the stationary state shown in Fig. 1(a), in contrast to the true ground state, more complicated flow pattern is stabilized. In this case, we observe two pairs of countercircling flows. The particle current consists of both the canonical part and the gauge part induced by the SOC, and thus the net particle current along the circle equals to zero.

Fig. 1(b) shows two examples of stationary states for the immiscible case with $g = 6000$, $g_{\uparrow\downarrow} = 8000$, $l = 5$, and $\kappa = 1.25$. For the immiscible case, the ground state for a uniform system is the stripe state, in which the two components are alternately aligned. For the toroidal trap, the direction of the stripe is almost in the same direction for a small central hole, and is along the ring in the limit of tight annulus [55]. For the stationary states shown in Fig. 1(b), interesting stripe patterns appear, such as vehicle wheel or flower petal patterns, which are quite different from usual ones. Similar but different patterns are obtained from run to run with different small initial noises, because there are an enormous number of different stationary states, whose energies are almost degenerate. Thus, we cannot determine the true ground state by the damped or imaginary-time GP evolution. The high degeneracy is due to the

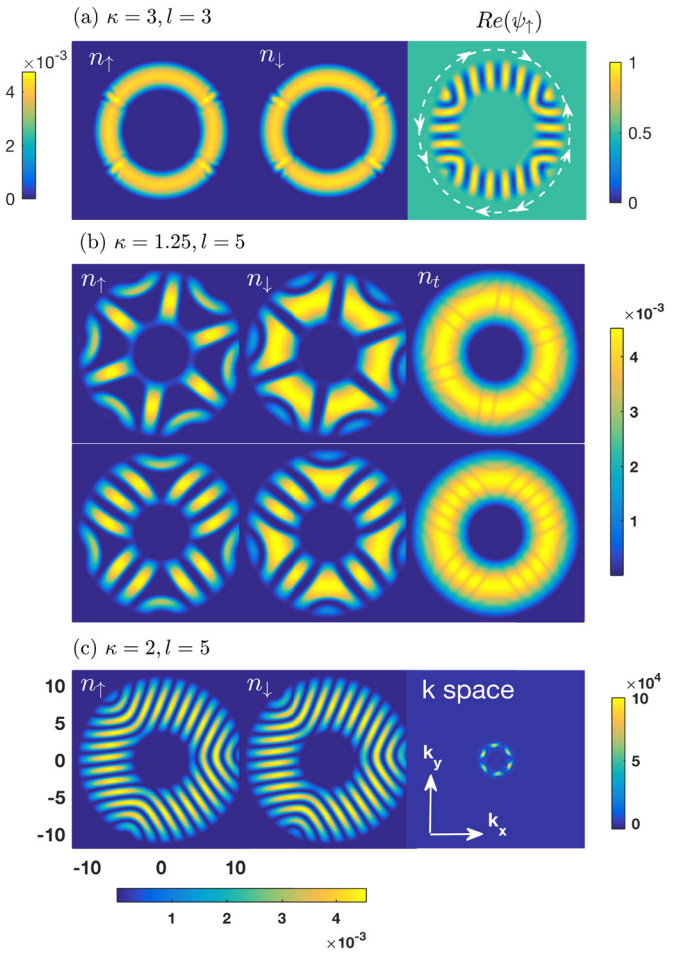

Fig. 1. (Color online.) Typical stationary states of a SO coupled BECs held under a toroidal trap for both miscible and immiscible cases. (a) The density and flow patterns for the miscible case with $g = 1000$, $g_{\uparrow\downarrow} = 800$, $A = 100$, $l = 3$, and $\kappa = 3$, where the direction of the mass flow is marked by the dashed-line arrows. (b) Two different types of density profiles for the immiscible case with $g = 6000$, $g_{\uparrow\downarrow} = 8000$, $A = 100$, $l = 5$, and $\kappa = 1.25$. (c) Density and momentum distributions for $\kappa = 2$, other parameters are the same as (b). The length is expressed in units of oscillator length $\sqrt{\hbar/(m\omega_\perp)}$, and the scale of each figure is 25.6×25.6.

competition between the nonlinear interaction, external potential, and SOC in this parameter regime.

Interestingly, with a further increase in SOC, the damped evolution always converges to a stationary state with triangular structure, as shown in Fig. 1(c) for $\kappa = 2.0$, although the true ground state is the stripe state aligned in the same direction. To get a deeper physical insight into the origin of this state, it is useful to look at its momentum distribution, which is presented in the third panel of Fig. 1(c). One can see that six maxima at angles $\varphi = \pi/3$ appear around the Rashba ring. This is in a sense reminiscent of the harmonically-trapped case, where a lattice phase emerges as the ground state [21]. In the present case, large l leads to a large radius of the toroidal trap and a large central hole, and the behavior of the system is intermediate between the harmonic potential and one-dimensional (1D) ring. As a result, the density distribution of the system shows the triangular stripe phase, where main region of the toroidal trap is occupied by the straight stripes and their vertices with an equilateral triangle shape by curved stripes.

We note that most of the initial states, including the ground state of the system without SOC and the totally random initial states, converge to the same or similar stationary states shown in Fig. 1 through the damped GP evolution. This strongly suggests that these stationary states can be obtained in real experiments.

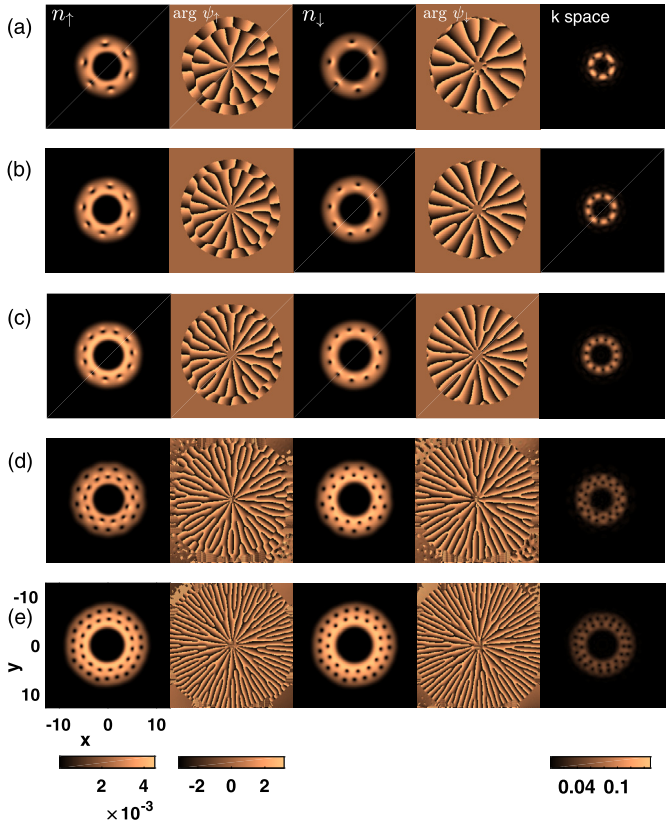

Fig. 2. (Color online.) Typical vortex structures of the rotating system for $l = 2$, and for rotation frequencies $\Omega = 0.4, 0.5, 0.6, 0.7$, and 0.8, corresponding to (a), (b), (c), (d) and (e), respectively. From left to right: density of up-component, phase of up-component, density of down-component, phase of down-component, and k-space density of the up-component. Other parameters are given as $g = 6000$, $g_{\uparrow\downarrow} = 8000$, $\kappa = 1.0$, and $A = 100$. The length is expressed in units of oscillator length $\sqrt{\hbar/(m\omega_\perp)}$, and the scale of each figure is 25.6×25.6.

Once these stationary states are formed, they can survive for a long time since there exists an energy barrier to decay into the true ground states. In addition, such 2D patterns can not survive in the limit of tight annulus. The density distribution of the system will shows an alternately arranged stripe pattern along the ring, and the number of stripes increases with the strength of the SOC [55].

3.2. Rotational property

One of the interesting aspects of the toroidal trap is its rotational property, which manifests itself as the presence of quantized vortices and its related vortex lattices [59,60]. The typical vortex structures of a harmonically-trapped BECs with SOC and rotation have been well studied, showing various exotic vortex lattices by varying the strength of SOC and rotation frequency [33–35,38].

Our numerical results show that when the rotation frequency Ω is small, vortices are distributed on a circle and the number of vortices along the circle increases with Ω, as shown in Figs. 2(a)-2(c) for $\Omega = 0.4, 0.5, 0.6$, respectively. We find that the vortices in up-component and down-component are slightly shifted from each other, which is due to the SOC [61]. The direction of the shift is in the radial direction, i.e., perpendicular to the direction of the flow, as reported in Ref. [61]. With an increase in the rotation frequency, we find that not only the number of vortices along a single circle but also the number of circles increases, as shown in Figs. 2(d)–2(e) for $\Omega = 0.7, 0.8$, respectively. Such circle-like alignment of vortices may be due to the anisotropic interaction between vortices due to the SOC [61], which merits further study.

For fixed l and Ω, either the number of vortices on each circle or the number of vortex circles increases with the strength of SOC, which is easily explained by the fact that the SOC can help vortex nucleation.

4. Conclusions

In summary, we have considered a rotating SO coupled BEC confined in a toroidal trap. In the absence of rotation, the stationary states of the system show exotic structures, such as vehicle wheel and flower-petal stripe patterns, which we attribute to the competitions between the external potential and SOC. For the miscible case, more complicated flow pattern can be formed in the stationary state compared with the countercircling one for the ground state. In the presence of rotation, the system is found to exhibit exotic ground-state vortex configurations by varying the strength of SOC and rotation frequency. In real experiments, both the strength of SOC and the shape of external potential can be controlled by optics means. Thus, we expect that the parameters used in this work are within current experimental capacity.

Acknowledgements

This work was supported by the National Natural Science Foundation of China under Grants No. 11775253, No. 11704383, No. 11505054, No. 11465009, and No. 61504016; by the Youth Innovation Promotion Association of CAS under Grant No. 2015334; by the Chongqing Research Program of Basic Research and Frontier Technology under Grant No. cstc2014jcyjA50016; by the JSPS KAKENHI Grant Numbers JP16K05505, JP17K05595, JP17K05596, and JP25103007; and by the Natural Science Foundation of Hunan Province under Grant No. 2018JJ3112.

References

[1] Y.J. Lin, R.L. Compton, K. Jiménez-García, J.V. Porto, I.B. Spielman, Synthetic magnetic fields for ultracold neutral atoms, Nature 462 (2009) 628–632.
[2] Y.J. Lin, K. Jiménez-García, I.B. Spielman, Spin–orbit-coupled Bose–Einstein condensates, Nature 471 (2011) 83–86.
[3] Y.J. Lin, R.L. Compton, K. Jiménez-García, W.D. Phillips, J.V. Porto, I.B. Spielman, A synthetic electric force acting on neutral atoms, Nat. Phys. 7 (2011) 531–534.
[4] Y.J. Lin, R.L. Compton, A.R. Perry, W.D. Phillips, J.V. Porto, I.B. Spielman, Bose–Einstein condensate in a uniform light-induced vector potential, Phys. Rev. Lett. 102 (2009) 130401.
[5] B.M. Anderson, G. Juzeliūnas, V.M. Galitski, I.B. Spielman, Synthetic 3D spin–orbit coupling, Phys. Rev. Lett. 108 (2012) 235301.
[6] P. Wang, Z.Q. Yu, Z. Fu, J. Miao, L. Huang, S. Chai, H. Zhai, J. Zhang, Spin–orbit coupled degenerate Fermi gases, Phys. Rev. Lett. 109 (2012) 095301.
[7] Z. Fu, L. Huang, Z. Meng, P. Wang, L. Zhang, S. Zhang, H. Zhai, P. Zhang, J. Zhang, Production of Feshbach molecules induced by spin–orbit coupling in Fermi gases, Nat. Phys. 10 (2014) 110–115.
[8] L. Huang, Z. Meng, P. Wang, P. Peng, S.L. Zhang, L. Chen, D. Li, Q. Zhou, J. Zhang, Experimental realization of two-dimensional synthetic spin–orbit coupling in ultracold Fermi gases, Nat. Phys. 12 (2016) 540–544.
[9] Z.M. Meng, L.H. Huang, P. Peng, D.H. Li, L.C. Chen, Y. Xu, C. Zhang, P. Wang, J. Zhang, Experimental observation of a topological band gap opening in ultracold Fermi gases with two-dimensional spin–orbit Coupling, Phys. Rev. Lett. 117 (2016) 235304.
[10] S.C. Ji, J.Y. Zhang, L. Zhang, Z.D. Du, W. Zheng, Y.J. Deng, H. Zhai, S. Chen, J.W. Pan, Experimental determination of the finite-temperature phase diagram of a spin–orbit coupled Bose gas, Nat. Phys. 10 (2014) 314–320.
[11] Z. Wu, L. Zhang, W. Sun, X.T. Xu, B.Z. Wang, S.C. Ji, Y. Deng, S. Chen, X.J. Liu, J.W. Pan, Realization of two-dimensional spin–orbit coupling for Bose–Einstein condensates, Science 354 (2016) 83–88.
[12] J.R. Li, J. Lee, W. Huang, S. Burchesky, B. Shteynas, F.C. Top, A.O. Jamison, W. Ketterle, A stripe phase with supersolid properties in spin–orbit-coupled Bose–Einstein condensates, Nature 543 (2017) 91–94.
[13] H. Zhai, Degenerate quantum gases with spin–orbit coupling: a review, Rep. Prog. Phys. 78 (2015) 026001.
[14] J. Dalibard, F. Gerbier Juzeliūnas, P. Öhberg, Colloquium: artificial gauge potentials for neutral atoms, Rev. Mod. Phys. 83 (2011) 1523–1543.
[15] N. Goldman, G. Juzeliūnas, P. Öhberg, I.B. Spielman, Light-induced gauge fields for ultracold atoms, Rep. Prog. Phys. 77 (2014) 126401.
[16] C. Wang, C. Gao, C.M. Jian, H. Zhai, Spin–orbit coupled spinor Bose–Einstein condensates, Phys. Rev. Lett. 105 (2010) 160403.
[17] H. Hu, B. Ramachandhran, H. Pu, X.J. Liu, Spin–orbit coupled weakly interacting Bose–Einstein condensates in harmonic traps, Phys. Rev. Lett. 108 (2012) 010402.
[18] B. Ramachandhran, B. Opanchuk, X.J. Liu, H. Pu, P.D. Drummond, H. Hu, Half-quantum vortex state in a spin–orbit-coupled Bose–Einstein condensate, Phys. Rev. A 85 (2012) 023606.
[19] T.L. Ho, S. Zhang, Bose–Einstein condensates with spin–orbit interaction, Phys. Rev. Lett. 107 (2011) 150403.
[20] C. Zhu, L. Dong, H. Pu, Harmonically trapped atoms with spin–orbit coupling, J. Phys. B 49 (2016) 145301.
[21] S. Sinha, R. Nath, L. Santos, Trapped two-dimensional condensates with synthetic spin–orbit coupling, Phys. Rev. Lett. 107 (2011) 270401.
[22] H. Sakaguchi, B. Li, B.A. Malomed, Creation of two-dimensional composite solitons in spin–orbit-coupled self-attractive Bose–Einstein condensates in free space, Phys. Rev. E 89 (2014) 032920.
[23] H. Sakaguchi, E.Ya. Sherman, B.A. Malomed, Vortex solitons in two-dimensional spin–orbit coupled Bose–Einstein condensates: effects of the Rashba–Dresselhaus coupling and Zeeman splitting, Phys. Rev. E 94 (2016) 032202.
[24] H. Sakaguchi, B.A. Malomed, Flipping-shuttle oscillations of bright one- and two-dimensional solitons in spin–orbit-coupled Bose–Einstein condensates with Rabi mixing, Phys. Rev. A 96 (2017) 043620.
[25] Y. Li, Z. Luo, Y. Liu, Z. Chen, C. Huang, S. Fu, H. Tan, B.A. Malomed, Two-dimensional solitons and quantum droplets supported by competing self- and cross-interactions in spin–orbit-coupled condensates, New J. Phys. 19 (2017) 113043.
[26] Y. Zhang, L. Mao, C. Zhang, Mean-field dynamics of spin–orbit coupled Bose–Einstein condensates, Phys. Rev. Lett. 108 (2012) 035302.
[27] Y. Li, L.P. Pitaevskii, S. Stringari, Quantum tricriticality and phase transitions in spin–orbit coupled Bose–Einstein condensates, Phys. Rev. Lett. 108 (2012) 225301.
[28] T. Kawakami, T. Mizushima, M. Nitta, K. Machida, Stable skyrmions in SU(2) gauged Bose–Einstein condensates, Phys. Rev. Lett. 109 (2012) 015301.
[29] E. Ruokokoski, J.A.M. Huhtamäki, M. Möttönen, Stationary states of trapped spin–orbit-coupled Bose–Einstein condensates, Phys. Rev. A 86 (2012) 051607.
[30] A.L. Fetter, Rotating trapped Bose–Einstein condensates, Rev. Mod. Phys. 81 (2009) 647–691.
[31] B. Dong, L.X. Wang, G.P. Chen, W. Han, S.G. Zhang, X.F. Zhang, Equilibrium vortex lattices of a binary rotating atomic Bose–Einstein condensate with unequal atomic masses, Ann. Phys. 373 (2016) 178–187.
[32] X.F. Zhang, W. Han, H.F. Jiang, W.M. Liu, H. Saito, S.G. Zhang, Topological defect formation in rotating binary dipolar Bose–Einstein condensate, Ann. Phys. 375 (2016) 368–377.
[33] X.Q. Xu, J.H. Han, Spin–orbit coupled Bose–Einstein condensate under rotation, Phys. Rev. Lett. 107 (2011) 200401.
[34] J. Radić, T.A. Sedrakyan, I.B. Spielman, V. Galitski, Vortices in spin–orbit-coupled Bose–Einstein condensates, Phys. Rev. A 84 (2011) 063604.
[35] X.F. Zhou, J. Zhou, C.J. Wu, Vortex structures of rotating spin–orbit-coupled Bose–Einstein condensates, Phys. Rev. A 84 (2011) 063624.
[36] A. Aftalion, P. Mason, Phase diagrams and Thomas–Fermi estimates for spin–orbit-coupled Bose–Einstein condensates under rotation, Phys. Rev. A 88 (2013) 023610.
[37] H. Sakaguchi, K. Umeda, Solitons and vortex lattices in the Gross–Pitaevskii equation with spin–orbit coupling under rotation, J. Phys. Soc. Jpn. 85 (2016) 064402.
[38] A.L. Fetter, Vortex dynamics in spin–orbit-coupled Bose–Einstein condensates, Phys. Rev. A 89 (2014) 023629.
[39] S. Eckel, J.G. Lee, F. Jendrzejewski, N. Murray, C.W. Clark, C.J. Lobb, W.D. Phillips, M. Edwards, G.K. Campbell, Hysteresis in a quantized superfluid 'atomtronic' circuit, Nature 506 (2014) 200–203.
[40] A.A. Wood, B.H.J. McKellar, A.M. Martin, Persistent superfluid flow arising from the He–McKellar–Wilkens effect in molecular dipolar condensates, Phys. Rev. Lett. 116 (2016) 250403.
[41] F. Jendrzejewski, S. Eckel, N. Murray, C. Lanier, M. Edwards, C.J. Lobb, G.K. Campbell, Resistive flow in a weakly interacting Bose–Einstein condensate, Phys. Rev. Lett. 113 (2014) 045305.
[42] L. Corman, L. Chomaz, T. Bienaimé, R. Desbuquois, C. Weitenberg, S. Nascimbéne, J. Dalibard, J. Beugnon, Quench-induced supercurrents in an annular Bose gas, Phys. Rev. Lett. 113 (2014) 135302.
[43] S. Beattie, S. Moulder, R.J. Fletcher, Z. Hadzibabic, Persistent currents in spinor condensates, Phys. Rev. Lett. 110 (2013) 025301.
[44] K.C. Wright, R.B. Blakestad, C.J. Lobb, W.D. Phillips, G.K. Campbell, Driving phase slips in a superfluid atom circuit with a rotating weak link, Phys. Rev. Lett. 110 (2013) 025302.
[45] C. Ryu, P.W. Blackburn, A.A. Blinova, M.G. Boshier, Experimental realization of Josephson junctions for an atom SQUID, Phys. Rev. Lett. 111 (2013) 205301.

[46] C. Ryu, M.F. Andersen, P. Cladé, V. Natarajan, K. Helmerson, W.D. Phillips, Observation of persistent flow of a Bose–Einstein condensate in a toroidal trap, Phys. Rev. Lett. 99 (2007) 260401.
[47] S. Bargi, F. Malet, G.M. Kavoulakis, S.M. Reimann, Persistent currents in Bose gases confined in annular traps, Phys. Rev. A 82 (2010) 043631.
[48] M. Abad, A. Sartori, S. Finazzi, A. Recati, Persistent currents in two-component condensates in a toroidal trap, Phys. Rev. A 89 (2014) 053602.
[49] A.M. Mateo, A. Gallemí, M. Guilleumas, R. Mayol, Persistent currents supported by solitary waves in toroidal Bose–Einstein condensates, Phys. Rev. A 91 (2015) 063625.
[50] R. Kanamoto, H. Saito, M. Ueda, Symmetry breaking and enhanced condensate fraction in a matter-wave bright soliton, Phys. Rev. Lett. 94 (2005) 090404.
[51] T. Shimodaira, T. Kishimoto, H. Saito, Connection between rotation and miscibility in a two-component Bose–Einstein condensate, Phys. Rev. A 82 (2010) 013647.
[52] A. Roussou, J. Smyrnakis, M. Magiropoulos, N.K. Efremidis, G.M. Kavoulakis, Rotating Bose–Einstein condensates with a finite number of atoms confined in a ring potential: spontaneous symmetry breaking beyond the mean-field approximation, Phys. Rev. A 95 (2017) 033606.
[53] H. Wang, L. Wen, H. Yang, C. Shi, J. Li, Vortex states and spin textures of rotating spin–orbit-coupled Bose–Einstein condensates in a toroidal trap, J. Phys. B 50 (2017) 155301.
[54] E.Ö. Karabulut, F. Malet, A.L. Fetter, G.M. Kavoulakis, S.M. Reimann, Spin–orbit-coupled Bose–Einstein-condensed atoms confined in annular potentials, New J. Phys. 18 (2016) 015013.
[55] X.F. Zhang, M. Kato, W. Han, S.G. Zhang, H. Saito, Vortex states and spin textures of rotating spin–orbit-coupled Bose–Einstein condensates in a toroidal trap, Phys. Rev. A 95 (2017) 033620.
[56] A.C. White, Y. Zhang, T. Busch, Odd-petal-number states and persistent flows in spin–orbit-coupled Bose–Einstein condensates, Phys. Rev. A 95 (2017) 041604.
[57] A. Ramanathan, K.C. Wright, S.R. Muniz, M. Zelan, W.T. Hill III, C.J. Lobb, K. Helmerson, W.D. Phillips, G.K. Campbell, Superflow in a toroidal Bose–Einstein condensate: an atom circuit with a tunable weak link, Phys. Rev. Lett. 106 (2011) 130401.
[58] M. Tsubota, K. Kasamatsu, M. Ueda, Vortex lattice formation in a rotating Bose–Einstein condensate, Phys. Rev. A 65 (2002) 023603.
[59] A. Aftalion, P. Mason, Rotation of a Bose–Einstein condensate held under a toroidal trap, Phys. Rev. A 81 (2010) 023607.
[60] M. Abad, Persistent currents in coherently coupled Bose–Einstein condensates in a ring trap, Phys. Rev. A 93 (2016) 033603.
[61] M. Kato, X.F. Zhang, H. Saito, Vortex pairs in a spin–orbit-coupled Bose–Einstein condensate, Phys. Rev. A 95 (2017) 043605.